Recent Results and Future Prospects of the
UA2 Experiment at the CERN p̄p Collider

The UA2 Collaboration
presented by H. Plothow-Besch

Institut für Hochenergiephysik der Universität
Heidelberg

INSTITUT FÜR HOCHENERGIEPHYSIK
UNIVERSITÄT HEIDELBERG

Recent Results and Future Prospects of the UA2 Experiment at the CERN $\bar{p}p$ Collider

The UA2 Collaboration
presented by H. Plothow-Besch

Institut für Hochenergiephysik der Universität
Heidelberg

RECENT RESULTS AND FUTURE PROSPECTS OF THE UA2 EXPERIMENT AT THE CERN p̄p COLLIDER

The UA2 Collaboration

presented by H. Plothow – Besch

IHEP, Heidelberg, FRG

1. INTRODUCTION

The CERN SPS p̄p Collider program[1] in the years 1981-1985 has been a great success and has given inportant contributions to the field of particle physics. Encouraged by such achievements and motivated by equally exciting physics topics still unrevealed and possibly within reach - the top quark and supersymmetry searches are just prominent examples - CERN has undertaken an important upgrading of the p̄p Collider complex[2].

In order to exploit the possibilities offered by the upgraded Collider facility, an improvement program was also undertaken since 1985 on the UA2 detector[3]. Emphasis was given to detect events with the emission of non interacting - particles with high transverse momentum such as neutrinos and to improve the electron identification. Furthermore, to cope with the expected increase in luminosity (by a factor of ~10) and with the amount of information available for each event, a new data acquisition and a more selective trigger system with three levels were implemented[4]. In Section 2 the motivations and the main aspects of the upgraded UA2 detector (for convenience, we will refer to it simply as UA2') are disscussed. Some of the main physics results reached so far with the UA2 detector are reviewed in Section 3 (topics related to the Standard Model) and in Section 4 (minimal extension to the Standard Model and search for exotics); the physics prospects for the near future that UA2' intends to address are also discussed. Finally, the experience gained with the new detector during the first run in November-December 1987 is reported in Section 5.

2. THE DETECTOR IMPROVEMENTS

2.1 Electron identification

One of the main goals of the UA2' experiment is the search for the top quark via its decay t → bev. Such electrons are expected to populate the low p_T region, where the data collected by the original UA2 detector were dominated by background from jets faking electrons. The two dominant background mechanisms were electron pairs from photon conversion and spatial overlaps of a low energy charged hadron with one or more high p_T

photons. In the upgraded detector, a hodoscope of Silicon counters (SI) reduces the background due to conversions by measuring dE/dx with a high granularity detector, while a Transition Radiation Detector (TRD) separates electrons from charged hadrons by detecting the X-rays emitted from particles with high γ ($\gamma = E/m_0$). A detailed description of the design and performance of these devices can be found in Ref. 5. The resulting rejection power against fake electrons is expected to increase by a factor of 25-30 with respect to UA2, as measured with electron and pion beams. The limited radial space available in UA2 and the relatively large overall thickness of the TRD have imposed the use of very compact tracking devices. These are a cylindrical drift chamber placed near the beam pipe, the Jet Chamber Vertex Detector (JVD), and a Scintillating Fiber Detector (SFD) just after the TRD and acting also as preshower detector in the central region. A general layout of the new UA2′ detector is shown in Fig. 1. Its components are briefly described in the next paragraphs. The UA2′ detector consists of

i. A cylindrical drift chamber of the "jet type" (JVD) to measure tracks close to the vertex, which surrounds a beryllium beam pipe. From test beam results the resolution of the JVD is expected to be about 0.15 mm in $R \times \phi$ and a 1 cm in z from charge division (strips on the outer layer provide a z resolution of 1 mm). With the present level of calibration the resolution on collider data is 0.35 mm and 3 cm respectively.

ii. A Silicon Hodoscope[6] made of 3024 40 × 8 mm pads, supported by a cylinder of 140 mm radius. The main functions of the silicon hodoscope are the rejection of gamma-conversion by dE/dx measurement and the removal of "ghost" tracks.

iii. A Transition Radiation Detector (TRD) fills the available radial space of 210 mm. It consists of two coaxial cylindrical chambers, each made of a stack of polypropylene radiators followed by a xenon chamber, which has a drift region followed by an amplification region. The X-ray photons produced by electrons in the converter are rapidly absorbed by the xenon in the early part of the chamber and generate large signals at late time with respect to the ones produced in the amplification region by any ionising particle. Signals are digitized by 100 Mhz FADCs[7]. The outer cathode of each chamber, made of helicoidal strips, is also connected to 15 Mhz FADCs enabling the charge induced by the sense wire avalanches to be measured.

iv. A Scintillating Fibre Detector[8] (SFD) provides track segments and the start of electromagnetic showers in front of the Central Calorimeter. It consists of about 60000 scintillating fibres, 1 mm in diameter, arranged in 24 coaxial cylindrical layers forming 8 stereo triplets. A lead converter, 1.5 radiation length thick, is inserted before the last two stereo triplets, all along the angular range covered by the central calorimeter. The fibres are read by means of 32 read-out chains, each consisting of three Image Intensifiers, one CCD and a FASTBUS digitizer, providing the necessary amplification, image demagnification, multiplexing and data compaction.

Tracking and electron identification in the forward regions are provided by a set of proportional tube chambers (ECPT) located in front of the new End-Cap calorimeters. The ECPT detector is described in Ref. 5, which also gives details of a fast time-of-flight system aimed at measuring the vertex position with good precision.
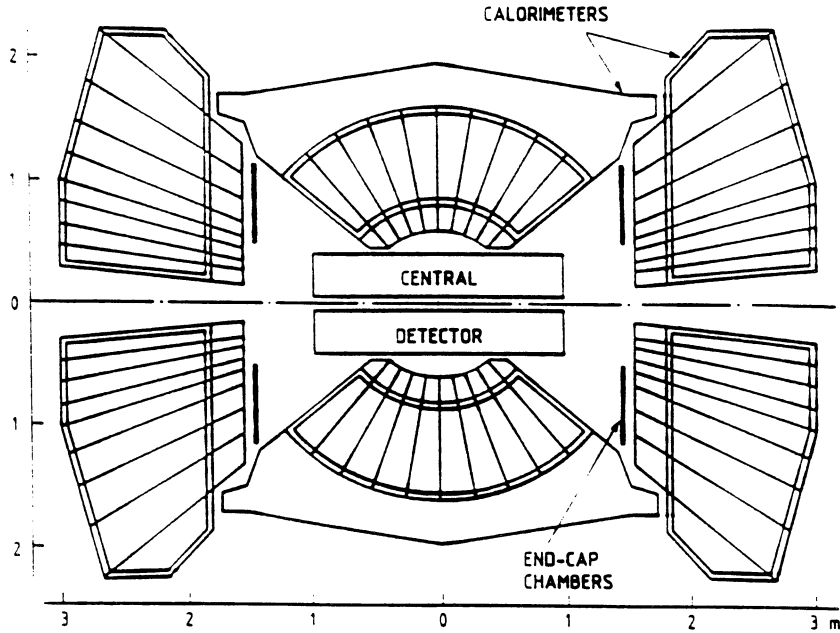
CALORIMETERS

Figure 1: Longitudinal view of the UA2′ detector

2.2 "Neutrino" Identification.

Non-interacting particles, such as neutrinos, among the final state products can in principle be detected by measuring the total transverse momentum vector associated to the visible particles. The missing transverse momentum vector is defined as $\vec{p}_T^{\,miss} = -\Sigma \vec{p}_T^{\,i}$, where $\vec{p}_T^{\,i}$ is a vector with magnitude given by the energy of the ith calorimeter cell and directed from the event vertex to the cell centre. The sum extends to all calorimeter cells. The quality of the $\vec{p}_T^{\,miss}$ measurement is a function of the angular coverage of the calorimeter. The UA2 apparatus had full calorimetry in the central region ($40° < \theta < 140°$) and only electromagnetic calorimeters between $20°$ and $40°$, while there was no detection of particles below $20°$. Such an incomplete coverage was detrimental to the calculation of the missing transverse momentum.

In UA2′ the central calorimeter (CC) is unchanged, while the forward regions have been equipped with new End Cap Calorimeters (EC) extending to $5°$ from the beam axis. The EC being of the same kind as the CC, uniform hadronic measurement is guaranteed from $5° < \theta < 175°$ over the full azimuth.

Preliminary results of the quality of the $\vec{p}_T^{\,miss}$ measurement in UA2′ during the 1987 run are summarized in Fig. 2. Since the two components of the $\vec{p}_T^{\,miss}$ vector are gaussian with the same $\sigma = \sigma_x = \sigma_y$, one can show that $dn/d(p_T^{\,miss})^2 \sim \exp[-(p_T/\Delta^2)]$, where $\Delta = \sqrt{2}\,\sigma$ depends on ΣE_T. Fig. 2 shows the trend of Δ as a function of ΣE_T, which can be parametrised (solid line) by $\Delta = 1.06\,(\Sigma E_T)^{0.404}$ GeV. The UA2′ performance is likely to improve with final energy calibration.
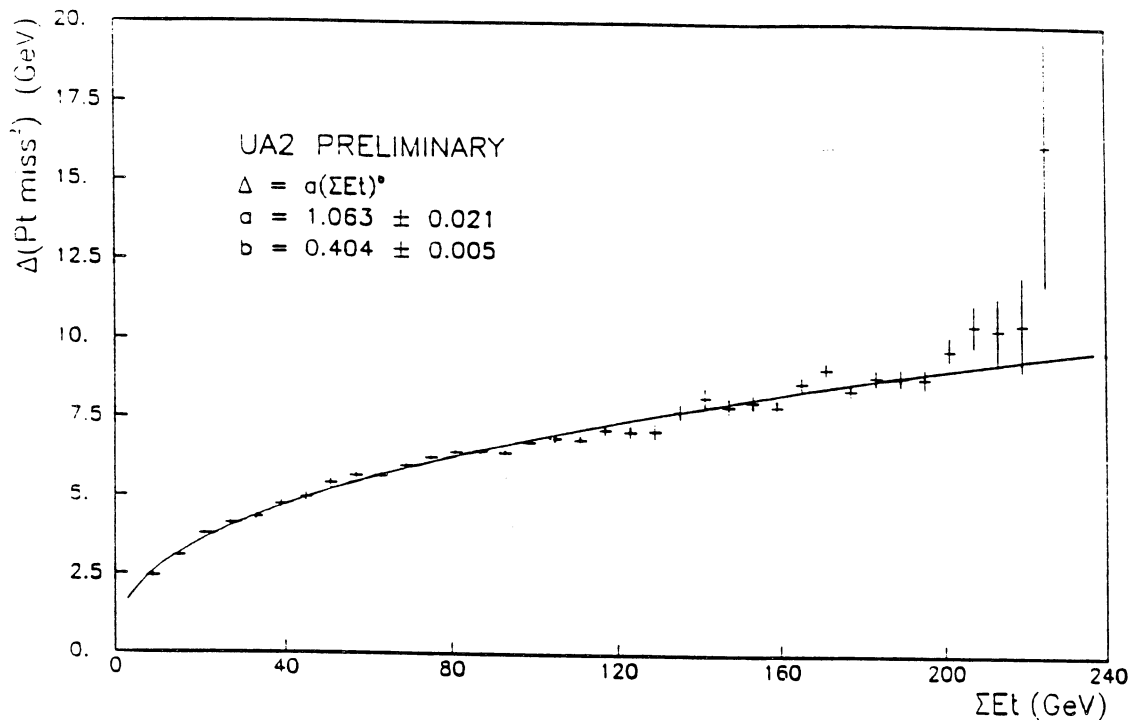
Figure 2: Resolution function of the transverse energy measurement in UA2'

3. THE PHYSICS - STANDARD MODEL.

3.1 W AND Z PHYSICS.

The accurate measurement of the Intermediate Vector Boson masses is of primary importance to test the Standard Model. While m_Z will be measured very accurately in the near future at SLC and LEP (we expect $\Delta (m_Z) \sim 50$ MeV/c^2), the W sector will remain the domain of $\bar{p}p$ Colliders until LEP Phase II.

3.1.1 Measurement of the W and Z masses.

The published results[9] from UA2 are based on 251 $W \to e\nu$ and 39 $Z \to e^+e^-$ decays, corresponding to an integrated luminosity of 910 nb^{-1}.
The mass values of W and Z measured by UA2 are:

i) $m_W = 80.2 \pm 0.6(\text{stat}) \pm 0.5(\text{syst}_1) \pm 1.3(\text{syst}_2)$ GeV/c^2

ii) $m_Z = 91.5 \pm 1.2(\text{stat}) \pm 1.7(\text{syst})$ GeV/c^2

as obtained by fitting i) the transverse mass distribution of the e-ν pair, $m_T^{e\nu}$, in events consistent with the reaction $\bar{p}p \to W + X \to e\nu + X$, ii) the mass distribution of the

e^+e^- pair in events consistent with the reaction $\bar{p}p \rightarrow Z + X \rightarrow e^+e^- + X$. The quoted systematic errors reflect uncertainties from the fit (syst$_1$) and from the knowledge of the calorimeter energy scale (syst$_2$).

For the upgraded UA2 detector with a total integrated luminosity of 10 pb^{-1}, $\sim$ 3000 $W \rightarrow e\nu$ and $\sim$ 350 $Z \rightarrow e^+e^-$ are expected. After applying fiducial cuts to select events with good energy measurement, the previous numbers will reduce to 2000-2500 and 200-250 respectively. The expected improvement in the measurement of m_W and m_Z is based on the following considerations.

i. With 10 pb^{-1} the expected statistical error is $\sim$ 220 MeV/c^2 for the W and $\sim$ 300 Mev/c^2 for the Z.

ii. The systematic error from the fit of the W mass depends on theoretical and experimental uncertainties on the width of the W, Γ_W, the production transverse momentum of the W, p_T^W, and the evaluation of p_T^ν through the measurement of p_T^{miss}. The uncertainty on Γ_W can be reduced by combining the measurements of the ratio $R_{exp} = \sigma_W^\ell/\sigma_Z^\ell$, at the CERN $\bar{p}p$ Collider, and of Γ_Z at LEP/SLC, where a precision of 30 MeV/c^2 is expected. The relation $\Gamma_Z/\Gamma_W = R_{exp}\,\sigma_Z/\sigma_W\,\Gamma_Z^\ell/\Gamma_W^\ell$ will give then Γ_W. The error from p_T^W would decrease by using p_T^Z from $Z \rightarrow e^+e^-$ to scale the theoretical calculation of p_T^W. Finally, the uncertainty on p_T^ν can be reduced by extracting m_Z with the same method used for m_W. It has been shown[9] that with high statistics the fit to the electron p_T distribution, sensitive to p_T^W but insensitive to p_T^ν, gives a more precise result than the one to $m_T^{e\nu}$, once the method just described to extract p_T^W is used. In this case, the expected systematic error from the fit of m_W is of the order of 200 MeV/c^2.

iii. The uncertainty on the knowledge of the energy scale (syst$_2$) is expected to improve from the 1.6% of UA2 to 1.0%, because of accurate beam calibrations and an improved calibration system of the UA2' calorimeters.

In conclusion, one expects an uncertainty of

$$\Delta m_W = \pm\ 0.22(\text{stat}) \pm 0.20(\text{syst}_1) \pm 0.80(\text{syst}_2)\ \text{GeV/c}^2$$
$$\Delta m_Z = \pm\ 0.30(\text{stat}) \pm 0.90(\text{syst})\ \text{GeV/c}^2.$$

The error on the energy scale, by far the dominant one, cancels to large extent in the ratio m_W/m_Z :

$$\Delta\ (m_W/m_Z) = \pm\ 0.003 \pm 0.002$$

Assuming then that m_Z will be measured with an accuracy of $\pm$ 50 MeV/c^2 at e^+e^- machines, the combination of $\bar{p}p$ Collider and LEP/SLC measurements will give

$$\Delta m_W = \pm\ 350\ \text{MeV/c}^2.$$

3.1.2 Standard Model Parameters.

The measurements of m_W and m_Z allow to check the predictions of the Standard Model, once properly renormalized and radiatively corrected quantities are used. In the scheme[10] where $\sin^2\theta_W$ is defined as

$$\sin^2\theta_W = 1 - (m_W/m_Z)^2 \qquad (1)$$

the SM predicts

$$m_W^2 = A^2/(1 - \Delta r) \sin^2\theta_W \qquad (2)$$
$$m_Z^2 = 4 A^2/(1 - \Delta r) \sin^2 2\theta_W \qquad (2')$$

where $A = \sqrt{(\pi\alpha/\sqrt{2} \, G_F)} = (37.2810 \pm 0.0003) \, GeV$ using the experimental measurements of the Fermi coupling constant and of the fine structure constant. The value of Δr, which accounts for one-loop radiative corrections at the W mass[11], is not constrained by experimental data. Recent calculations[12], based on a value for the top mass of 45 GeV/c^2 and for the Higgs of 100 GeV/c^2 give $\Delta r = 0.0711 \pm 0.0013$.

The Standard Model can be tested by extracting i) $\sin^2\theta_W$, ii) ρ, iii) Δr from the measured values of m_W and m_Z as follows :

i. Equation (1) provides a direct measurement of $\sin^2\theta_W$ independent of other experiments and of theoretical uncertainties. UA2 finds

$$\sin^2\theta_W = 0.232 \pm 0.025(\text{stat}) \pm 0.010(\text{syst})$$

where the systematic error is mostly related to the m_W fit, the mass scale uncertainty cancelling out in the ratio m_W/m_Z. In UA2' using (1) and for 10 pb^{-1}, we expect

$$\Delta(\sin^2\theta_W) = \pm 0.006(\text{stat}) \pm 0.004(\text{syst}).$$

A more precise value of the weak mixing angle can be extracted by a simultaneous fit of the measured m_W and m_Z to the theoretical equations (2) and (2'). The UA2 result is

$$\sin^2\theta_W = 0.232 \pm 0.003(\text{stat}) \pm 0.008(\text{syst})$$

where now the systematic error is dominated by the error on the mass scale and the measurement relies on other experimental results and theoretical calculations [respectively A and Δr in (2) and (2')]. The expected precision of this measurement in UA2' is :

$$\Delta(\sin^2\theta_W) = \pm 0.001(\text{stat}) \pm 0.005(\text{syst})$$

ii. Any departure from the Minimal Standard Model would result in modifications to the formalism presented above. In particular values of $\sin^2\theta_W$ from (1),(2) and from low-energy neutrino experiments would in general differ. Although all existing

measurements are in agreement with the Standard Model, they can be used to place limits on possible deviations from the Minimal Standard Model. In particular, the quantity $\rho = m_W^2/m_Z^2 \cos^2\theta_W$ is expected to be 1 in the Minimal Standard Model. UA2 measures

$$\rho = 1.001 \pm 0.028(\text{stat}) \pm 0.006 \text{ (syst)}$$

while the sensitivity of UA2′ is expected to be

$$\Delta\rho = \pm 0.008(\text{stat}) \pm 0.009(\text{syst}).$$

iii. The radiative correction parameter Δr can also be extracted from the measured values of m_W and m_Z. Eliminating $\sin^2\theta_W$ from (2) and (2′) the UA2 result is

$$\Delta r = 0.068 \pm 0.087(\text{stat}) \pm .030(\text{syst})$$

while using $\sin^2\theta_W$ from low-energy experiments we get

$$\Delta r = 0.068 \pm 0.022(\text{stat}) \pm 0.032(\text{syst}).$$

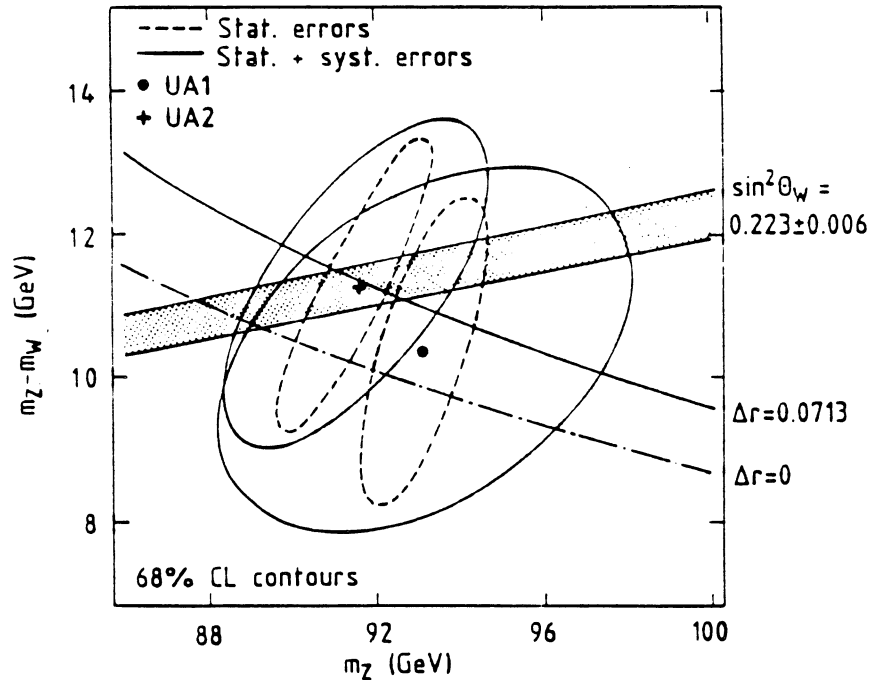This result can be visualised in the m_Z versus m_Z-m_W plane (Fig. 3).

Figure 3: m_Z versus m_Z - m_W. The 68% CL clipses represent the CERN Collider measurements and are compared with other results and expected SM values.

The present measurements, although in good agreement with the Standard Model, are not precise enough to test the presence of Δr. The expected sensitivity at the upgraded CERN $p\bar{p}$ Collider is summarized in Fig. 4, from which we can conclude that UA2' will test radiative corrections, once a precise measurement of m_z will be available from SLC or LEP.
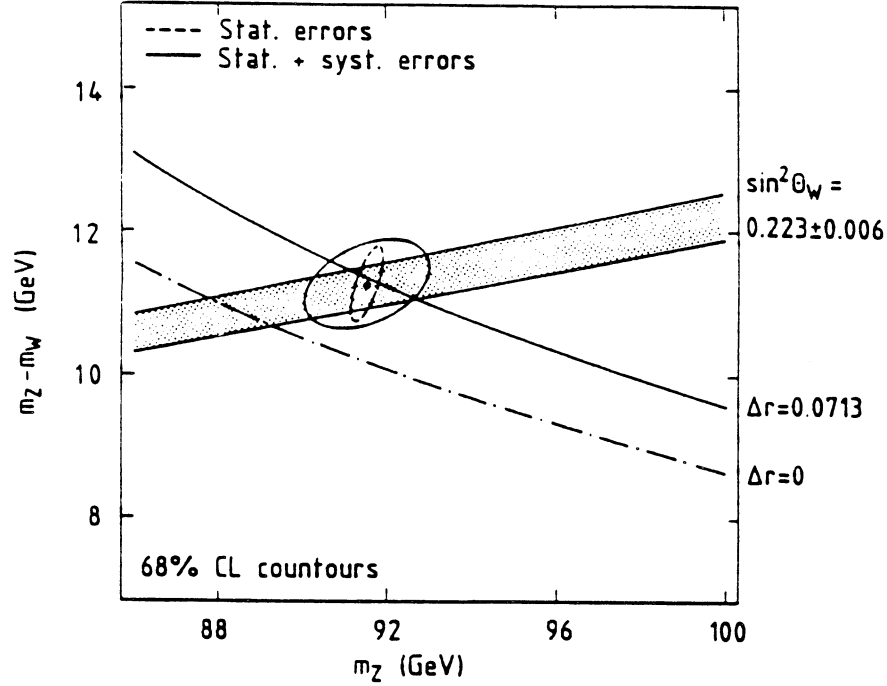

Figure 4: m_Z versus $m_Z - m_W$. The 68% CL elipses represent the expected ACOL results and are compared with other results and expected SM values.

The importance of a precise measurement of Δr resides in the fact that Δr would deviate from the computed value[12] if a new fermion family existed with a large mass splitting, or if there were additional gauge bosons, or again if the top quark were very heavy.

3.2 SEARCH FOR THE TOP QUARK.

At $p\bar{p}$ Colliders the main mechanisms of top production are via W production, if kinematically allowed, with the W decaying subsequently into $W \to t\bar{b}$, and QCD production of $p\bar{p} \to t\bar{t} + X$ via $q\text{-}\bar{q}$ annihilation or gluon-gluon fusion. At $\sqrt{s} = 630$ GeV the first reaction is the dominant one for top masses in the range of $40 < m_{top} < 80$ GeV/c^2. The production cross section can be precisely estimated through the relation

$$(W \to t\bar{b}) = 3\ \sigma(W \to e\nu)\ \phi(m_t)$$

where $\sigma(W \rightarrow e\nu)$ has been measured at the CERN Collider, $\phi(m_t)$ is a known phase space suppression term and the factor of 3 is for colour. Outside the above mass range, top production is dominated by direct $t\bar{t}$ production (2). A recent complete calculation of the next-to-leading order QCD corrections to the total cross-section for heavy flavour production[13] and a set of proton structure functions including the latest experimental results[14] has allowed the authors of Ref. 15 to give reliable predictions for top production.

Top decay proceeds through virtuel W exchange as

$$t \rightarrow (Wb) \rightarrow 3 \text{ jets} \quad \text{or} \quad t \rightarrow (Wb) \rightarrow \ell\nu + \text{jet.}$$

The final state will therefore consist of more than 4 jets or a charged lepton accompanied by two or more jets in events with missing transverse energy. Given the high rate of multi-jet events from QCD processes, the interesting final state at $\bar{p}p$ Colliders is the one connected to the semi-leptonic decay modes which, at the price of a branching ratio of 1/9 for each charged lepton, give a much cleaner signature.

The analysis requires very strict selection criteria, in order to improve the signal to background ratio. With the standard UA2 electron cuts[9] about 10 top events are expected over a background of 300 in the existing UA2 data sample. Strong requirements of electron isolation, both in tracking and preshower detectors and in the calorimeters, are necessary to improve the signal-to-background ratio. In this case, for an expectation of 3-4 events UA2 finds 30 candidates in the 910 nb^{-1} data sample, entirely consistent with background, both in rate and event topology.

The greatly improved electron identification power of UA2' should allow the detection of the top at the CERN $\bar{p}p$ Collider if its mass is smaller than the W mass. For 10 pb^{-1} we estimate that about 70 events containing a $t \rightarrow be\nu$ are expected, over a background of about 10 events, if $m_t = 40$ GeV/c^2, where the contributions from $W \rightarrow t\bar{b}$ and $t\bar{t}$ are about equal. For $m_t = 60$ GeV/c^2 the contribution from $t\bar{t}$ is about 25% of the total and the predicted signal is 20 events with a background of 4 events. For top masses approaching m_W the b jets are softer and therefore it becomes more and more difficult to distinguish $W \rightarrow t\bar{b}$ from W + jets production. On the other hand for the same kinematical reasons the $t\bar{t}$ channel will result in a final state containing a $\ell\nu$ and a two-jet pair with invariant masses close to m_W. Finally for $m_t > m_W$ the most promising channel is $t\bar{t} \rightarrow W^+W^-b\bar{b}$ followed by a semileptonic decay of one W. For $m_t = 100$ GeV/c^2, for example, about 10 events are expected before any selection cut necessary to reduce the background of W + two-jet production. We can consider, therefore, $m_t = 100$ GeV/c^2 as an (optimistic) upper limit of the sensitivity of top search in UA2'.

3.3 QCD MEASUREMENTS.

Among the many tests of QCD already made by UA2, only one topic will be briefly mentioned here.

3.3.1 Measurement of α_S.

In perturbative theory QCD predicts the occurence of gluon bremsstrahlung as first order perturbative correction in the strong coupling constant α_S to the parton-parton scattering. Final states containing three jets should be observed at a rate dependent on the value of α_S. Therefore, the yield of three-jet relative to two-jet events gives a measure of $\alpha_S \, k_3/k_2$. Unfortunately the contributions k_3 and k_2 from higher order corrections in α_S to the two and three-jet cross-sections have not been calculated yet and only the quantity $\alpha_S \, k_3/k_2$ can be extracted with this method. UA2 finds[16] $\alpha_S \, k_3/k_2 = 0.23 \pm 0.01 \pm 0.04$.

A similar approach consists in using the yield R of the W + jet relative to W production. By fitting the prediction of a QCD Monte Carlo[17] to the measured value of R, one can extract the value $\alpha_S \, k_1/k_0$, where the k factors take into account the corrections of higher order diagrams to the W + jet and W cross-sections, respectively. The advantage of this method is given by a recent evaluation[18] of k_0 and k_1 which allow to extract an absolute value for α_S. A final analysis on the UA2 data[19] gives

$$\alpha_S \, (m_W) = 0.13 \pm 0.03 (\text{stat}) \pm 0.03 (\text{syst}_1) \pm 0.02 (\text{syst}_2)$$

where syst_1 is the experimental error and syst_2 takes into account theoretical uncertainties.

Some of these uncertainties, such as the one related to the knowledge of the energy scale or the effect of the underlying event, will improve in UA2'. Taking into account statistical error corresponding to an integrated luminosity of 10 pb^{-1}, the overall error on the determination of α_S in UA2' with this method is expected to be of the order of $\Delta \alpha_S = 0.015 - 0.020$.

4. EXTENSIONS OF THE MINIMAL STANDARD MODEL.

4.1 New electroweak gauge bosons.

Additional vector bosons arise from any extension of the minimal SU(2)xU(1) group of the Standard Model, composite models or models derived from Superstring theories.

At $\bar{p}p$ Colliders they would be produced through $q\bar{q}$ annihilation and they would be detected via their leptonic decay, the decay into quarks being dominated by the two-jet background from QCD processes. the sensitivity of experiments is a function of their masses, $m_{W'}$ and $m_{Z'}$, their coupling to quarks and their branching ratio to leptons.

A search in UA2 excludes at a 90% confidence level the existence of a W' of $m_{W'} < 209 \text{ GeV/c}^2$ and a Z' of $m_{Z'} < 180 \text{ GeV/c}^2$, in the mass region above $m_{W'}$ and $m_{Z'}$ and for standard coupling to quarks and electrons. Details of the analysis, variation of the limits for different couplings and for masses around and below $m_{W'}$ and $m_{Z'}$ can be found in Ref. 20.

The sensitivity of UA2' at ACOL will be about 300 GeV/c^2 for $m_{W'}$ and 250 GeV/c^2 for $m_{Z'}$, for an integrated luminosity of 10 pb^{-1}.

4.2 SEARCH FOR EXOTICS - Supersymmetric particles.

Among the many mechanisms proposed to overcome the theoretical difficulties associated to the Higgs sector of the Standard electroweak theory, Supersymmetry seems to be the most far-reaching, since it provides a natural framework for spontaneously broken gauge theories involving elementary scalars. At $\bar{p}p$ Colliders the highest cross sections, for any given mass of the supersymmetric particles, would be for the strongly interacting ones, the squark $\tilde{q}$ and the gluino $\tilde{g}$, the dominant production channels being $\bar{p}p \rightarrow \tilde{g}\tilde{g}$, $\bar{p}p \rightarrow \tilde{g}\tilde{q}$, $\bar{p}p \rightarrow \tilde{q}\tilde{q}$. The subsequent decay depends on the relative values of the squark mass, $m_{\tilde{q}}$, with respect to the gluino mass, $m_{\tilde{g}}$: i) $\tilde{q} \rightarrow q\tilde{g}$, $\rightarrow q\bar{q}\tilde{\gamma}$ if $m_{\tilde{q}} > m_{\tilde{g}}$, or ii) $\tilde{g} \rightarrow \tilde{q}q$, $\tilde{q} \rightarrow q\tilde{\gamma}$ if $m_{\tilde{q}} < m_{\tilde{g}}$. Since in most models the photino is the lightest, non-interacting SUSY particle, the final states would consist in many (2 to 6) jets and p_T^{miss}. At the $Sp\bar{p}S$ Collider the UA1 detector was better placed than UA2 for the study of such configurations due to its larger η-coverage.

The better granularity of UA2 allowed to study the case of an unstable photino which, through the decay $\tilde{\gamma} \rightarrow \gamma\tilde{H}$, would produce a final state with two photons and jets[20]. The absence of events with a two-photon pair with invariant mass larger than 10 GeV/c^2 and at least two jets with $p_T > 10$ GeV/c translates into the following limits: UA2 excludes gluinos in the mass range 15 - 50 GeV/c^2 and squarks in 9 - 46 GeV/c^2.

UA2' will take advantage of the improved p_T^{miss} measurement and of the increased acceptance. Assuming a selection efficiency of 10% the sensitivity to scalar quarks and gluinos for L = 10 pb^{-1} should reach mass values of the order of 100 GeV/c^2.

5. THE FIRST RUN OF UA2'.

Many of the solutions adopted in the upgrading of the original UA2 detector have been constrained by the tight schedule imposed by the improvement program of the $\bar{p}p$ complex and the choice of being ready with the full configuration for the starting of the improved machine. All the detectors of the substantially modified apparatus have been successfully operational through the whole $\bar{p}p$ running period in November and December 1987 and preliminary results on their performance have been reported in Section 2. Unfortunately, technical problems both in the AA/AC and in the SPS resulted in a poor performance of the Collider, with a peak luminosity never exceeding 3×10^{29} cm^{-2}sec^{-1}, the same as the old machine, and a tiny integrated luminosity of 46 nb^{-1}, only 5% of the one accumulated so far by UA2. None of the problems have been of fundamental nature and have already been overcome in the actual running period of autumn 1988, when luminosities close to the design value of 4×10^{30} cm^{-2}sec^{-1} have been reached.

One major item in the UA2 upgrading, as mentioned in section 2, is indeed related to the capability of the experiment to face the expected high luminosity and the large data volume generated by the sophisticated UA2' detectors, i.e. the trigger and the data acquisition (DAQ) systems[4]. Two additional levels of software triggers were added to the hardware trigger of UA2. The DAQ system itself had to be upgraded to provide two stages of event processing and buffering. At the design luminosity of the upgraded $\bar{p}p$ Collider the expected rate from the first level trigger will be of the order of 100 Hz and the amount of data to be collected per event will average 80-100 kBytes. Several special

runs were made to simulate running conditions at 4×10^{30}cm^{-2}sec^{-1} and test the performance of the trigger and DAQ systems. No particular problems were detected. From the data accumulated so far (the available statistics has already been doubled) new results should be expected in the near future.

ACKNOWLEDGEMENT

REFERENCES

1. The Staff of the CERN Proton-Antiproton Project, Phys. Lett. **107B** (1981) 306.
2. E. Jones, Proc of the 6th Topical Workshop on Proton-Antiproton Collider Physics, Aachen, 1986, World Scientific, Singapore (1987), pp. 691.
3. UA2 Collaboration, "Proposal to Improve the Performance of the UA2 Detector" CERN/SPSC 84-30 SPSC/P93 Add.2 (1984);
   UA2 Collaboration, "Proposal to Improve the Performance of the UA2 Central Detector" CERN/SPSC 84-95 SPSC/P93 Add.3 (1984).
4. G. Blaylock et al., Proceedings of the International Conference on the impact of digital microelectronics and microprocessors on particle physics, ICTP, Trieste 1988.
5. UA2 Collaboration, C. Booth, Proc. 6th Topical Workshop on Proton-Antiproton Collider Physics, Aachen 1986, World Scientific, Singapore (1987) 381.
6. K. Borer et al., Nucl. Inst. Meth. **253A** (1987) 548.
7. F. Bourgeois, Nucl. Inst. Meth. **219A** (1984) 153.
8. R.E. Ansorge et al., Nucl. Inst. Meth. **265A** (1988) 33.
9. UA2 Collaboration, R. Ansari et al., Phys. Lett. **186B** (1987) 440;
   UA2 Collaboration, R. Ansari et al., Phys. Lett. **194B** (1987) 158. See references therein for previous UA2 publications.
10. W.J. Marciano and A. Sirlin, Phys Rev. **D29** (1984) 945.
11. W.J. Marciano, Phys Rev. **D20** (1979) 274;
    A. Sirlin, Phys Rev. **D22** (1980) 971;
    F. Antonelli et al., Phys. Lett. **91B** (1980) 90;
    M. Veltman, Phys. Lett. **91B** (1980) 95.
12. F. Jegerlehner, Z. Phys. **C32** (1986) 425.
13. P. Nason et al., Nucl. Phys. **B303** (1988) 607.
14. M. Diemoz et al., Z. Phys. **C39** (1988) 21.
15. G. Altarelli et al., Nucl. Phys. **B308** (1988) 724.
16. UA2 Collaboration, J.A. Appel et al., Z. Phys. **C30** (1986) 341.
17. S.D. Ellis et al., Phys. Lett. **154B** (1985) 435.
18. A.C. Bawa and W.J. Stirling, Durham preprint DPT/87/42 (1987).
19. UA2 Collaboration, R. Ansari et al., Phys. Lett. **215B** (1988) 175.
20. UA2 Collaboration, R. Ansari et al., Phys. Lett. **195B** (1987) 613.